NT-MDT Spectrum Instruments

Optical Imaging and Spectroscopy on the Nanometer Scale

SNOM applications in the following areas are presented:

- *Laser emission*
- *Optical fibers*
- *Optical micro-devices Plasmonics*
- *Photonic crystals and waveguides*
- *Photovoltaics*
- *Polymers*
- *Quantum Dots*
- *Scattering (Apertureless-) SNOM*

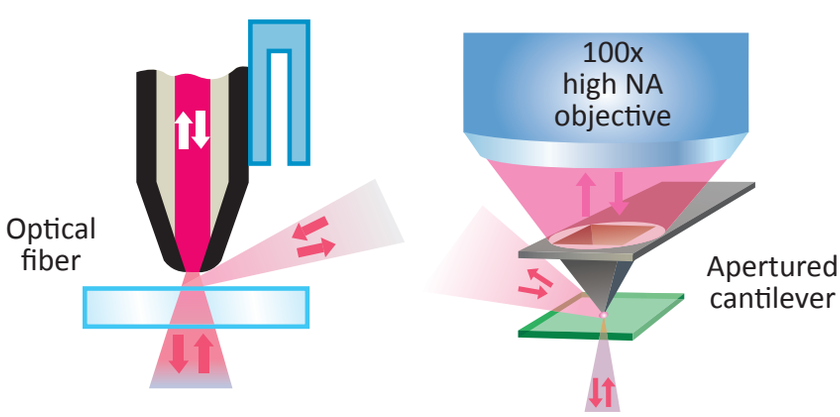

SNOM based on quartz fibers

SNOM based on silicon cantilevers with nanofabricated aperture

Scanning near-field optical microscopy (SNOM) enables studying a sample's optical properties with resolution far beyond the diffraction limit. Sample fluorescence, light emission, transmission, scattering etc. can be mapped with the spatial resolution down to tens of nanometers.

Two main approaches to the near-field microscopy exist: (i) aperture type SNOM and (ii) apertureless techniques.

In the first case, a subwavelength size aperture on a scanning tip is used as an optical probe. This is usually an opening in a metal coating of either an optical fiber tip or of a cantilever. Spatial resolution in the aperture type SNOM is, in general, determined by the aperture diameter.

Apertureless techniques are based on the near-field optical phenomena as well, but do not require passing the light through an aperture. Apertureless/Scattering SNOM, Tip Enhanced Raman/Fluorescence, STM Light Emission and others fall into this category.

SNOM techniques are widely used in nanophotonics (plasmonics, photonic crystals & waveguides etc.), laser technology, optical micro-devices and material science.

NT-MDT SI SNOM FEATURES

All major types of SNOM probes and measuring modes supported

Apertured cantilevers, different types and shapes of apertured optical fibers and even sharpened metal wires can be used as SNOM probes. Major SNOM measuring modes are: Transmission, Collection and Reflection. Signals measured: laser intensity, fluorescence intensity and full emission spectra.

Apertureless techniques: Scattering SNOM, Tip Enhanced Raman/Fluorescence and others

In general, all types of optical, mechanical, and electrical interactions between the probe, sample and incident light source can be studied by NT-MDT SI SNOM setup.

HybriD optical measuring mode:

In this mode tip-sample distance is periodically modulated. Tip gets in and out contact with the sample thousand times per second. Optical signal resulting from the tip-sample interaction is continuously measured and recorded for each approach-retract cycle by fast electronics. The resulting multi-dimensional data (optical signal vs. tip-sample distance in each XY scanning point) presents, upon proper post-processing, unique information about near-field and far-field components of the optical signal. This allows increasing SNOM measurement sensitivity and resolution.

Scanning by sample and/or by probe

Depending on the type of sample and measurement, it is important to have the option to scan either by the sample or by the probe to obtain SNOM images.

Environmental control (temperature, gases, humidity, liquid and external magnetic field)

Temperature control and air flow isolation are the key issues for measurements stability. Sample heating and controlled gas atmosphere removes the residual water layer on the sample (this is usually present in ambient conditions and affects any surface measurements). This prevents unwanted chemical reactions on the surface and other measurement artifacts.

Extended spectral region (UV – Vis – IR)

Standard supported wavelength range is 400-1700 nm. Customized solutions for wider ranges are possible.

Easy integration with AFM & confocal Raman microscopy

Universal NT-MDT SI NTEGRA SPM base allows one to switch easily between any types of AFM/STM/SNOM measuring heads and environmental cells. The setup can be further integrated with a Raman spectrometer to provide simultaneous AFM/Confocal Raman & fluorescence imaging in addition to SNOM.

SNOM IMAGING FOR LASER STUDIES

Study of Laser Emission Properties

SNOM can be effectively used to study laser emission properties. Both near-field (right at the laser facet) and far-field (at a certain distance from the facet) emission patterns can be obtained with high spatial resolution (<50 nm). Both emission intensity and full emission spectrum can be recorded during a 2D or 3D optical scan.

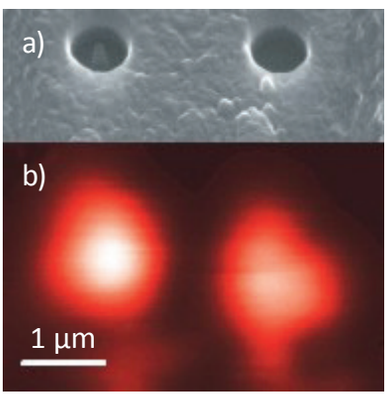

Fig. 1. (a) Side view SEM image of a verysmall-aperture-laser (VSAL) facet with an annular aperture (left) and a circular aperture (right). (b) Intensity distribution of the light emission (at 650 nm) detected at the surface of the VSAL facet.
Data from: Hongfeng Gai, Jia Wang, APPLIED OPTICS, Vol. 46, No. 25, 1 September 2007.

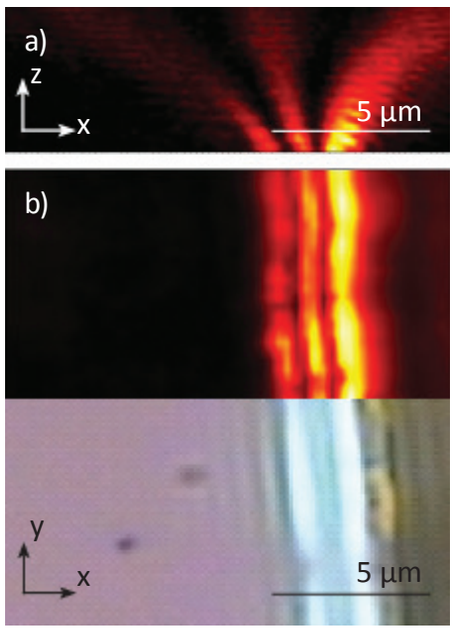

Fig. 2. (a) XZ section of the intensity distribution of the light emission (at ~1070 nm wavelength) from 0 to 4.5 µm above the surface of a cleaved laser. (b) Near-field intensity distribution of the light emission detected at the surface (top half) and optical image of cleaved laser (bottom half).
Data from: A. Shelaev, M. Yanul, NT-MDT SI.
Sample courtesy: A. Ankudinov, S. Slipchenko, A. Podoskin, I. Tarasov, Ioffe Physical Technical Institute.

SNOM FOR OPTICAL FIBERS

Broadband Emissions from γ-AL2O3 Nanocrystals in Cr-Doped Double-Clad Fibers

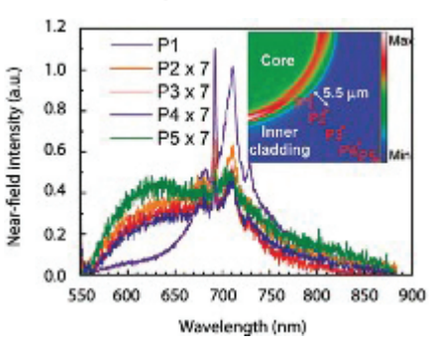

Fig. 3. Near-field spectra and corresponding SNOM mapping of the inner cladding and core of the Cr-doped double-clad fiber. The spectra show the broadband properties, their bandwidth and intensity, which are of concern for a potential optical coherence tomography light source. These spectra present the dependence on the radial distributions of Cr3+:γ-Al2O3 anocrystals and clusters.
Data from: Chien-Chih Lai, Shih-Chang Wang, Yen-Sheng Lin, Ting-Hao Chen, and Sheng-Lung Huang, JOURNAL OF PHYSICAL CHEMESTRY C, 115, 20289–20294 (2011).

Photonic Crystal Optical Fiber

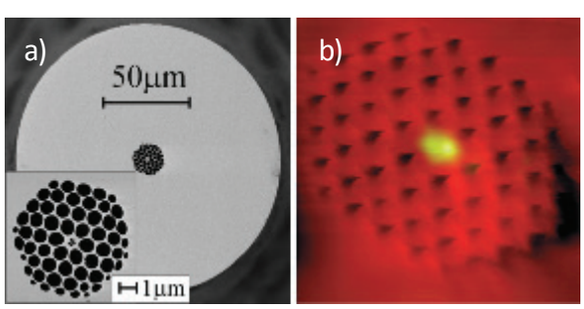

Fig. 4. (a) SEM image of the optical fiber cross-section, showing photonic crystal structure in the fiber core. (b) Overlay of topography map (red palette) and light intensity (SNOM collection) image (green palette) taken from the fiber section. Light propagating in the fiber is perfectly localized in the center of the photonic crystal structure.
Data from: Yinlan Ruan, Heike Ebendorff-Heidepriem, Tanya M. Monro, Centre of Expertise in Photonics, School of Chemistry & Physics, University of Adelaide.

Near-field Focusing of a Phase Micro-Fresnel Zone Plate

Focusing behavior of a binary phase micro-Fresnel zone plate (FZP) fabricated using focused ion beam milling on a glass substrate is studied by SNOM. It is found that an asymmetric spot with subwavelength beam width and elongated depth of focus can be obtained from the phase micro-FZP. The measurements are consistent with calculation results.

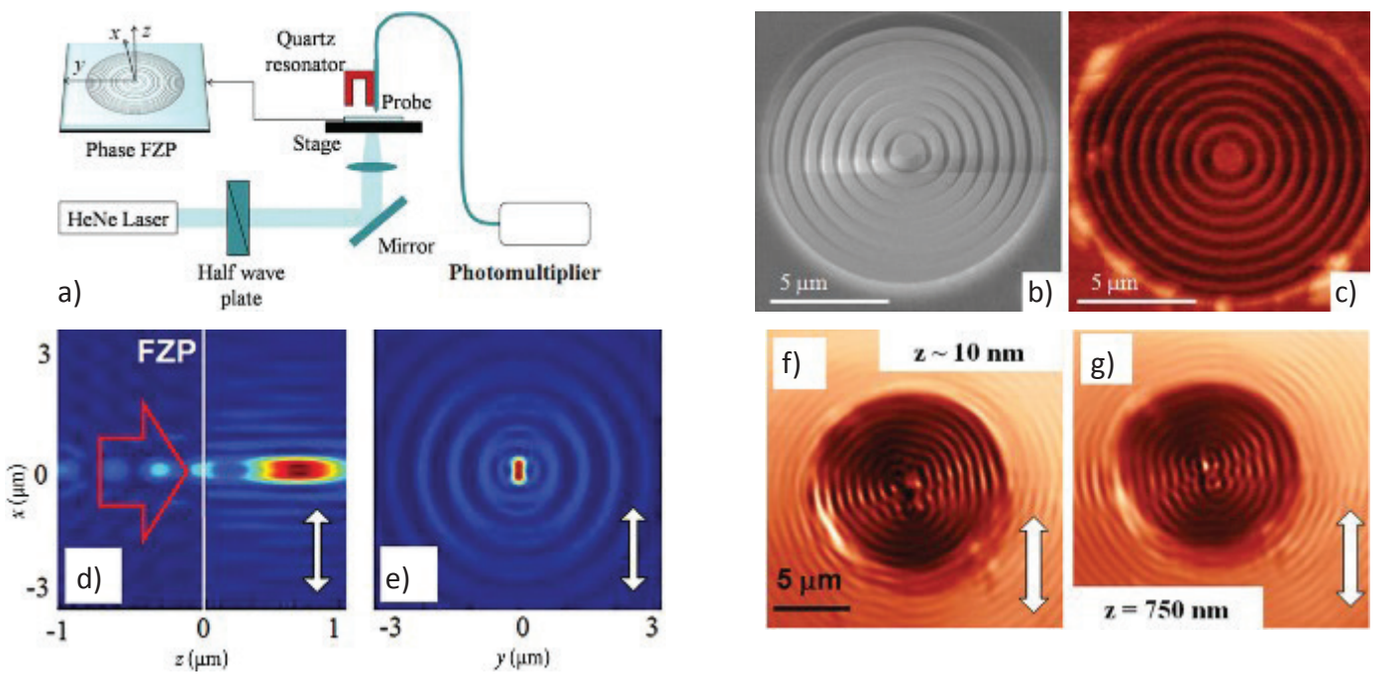

Fig. 5. (a) Experimental setup. (b) SEM image and (c) shear-force topography of the phase micro-FZP. The phase plate has eight full zones with the etch depth about 300 nm. (d), (e) Calculated electric field intensity distribution of the incident and transmitted lights in XZ and XY plane. (f), (g) Experimental intensity distribution of the electric field intensity (detected by SNOM) after being transmitted through the phase micro-FZP at planes located at 10 nm and 750 nm height from the plate surface.
Data from: R.G. Mote, S.F. Yu, A. Kumar, W. Zhou, X.F. Li, APPLIED PHYSICS B 102: 95–100 (2011).

Characterization of a Micro-focusing Plasmonic Device

Focusing behavior of Au based focusing plasmonic device is characterized by SNOM. The experimental results show a significant focusing effect in agreement with the simulation results.

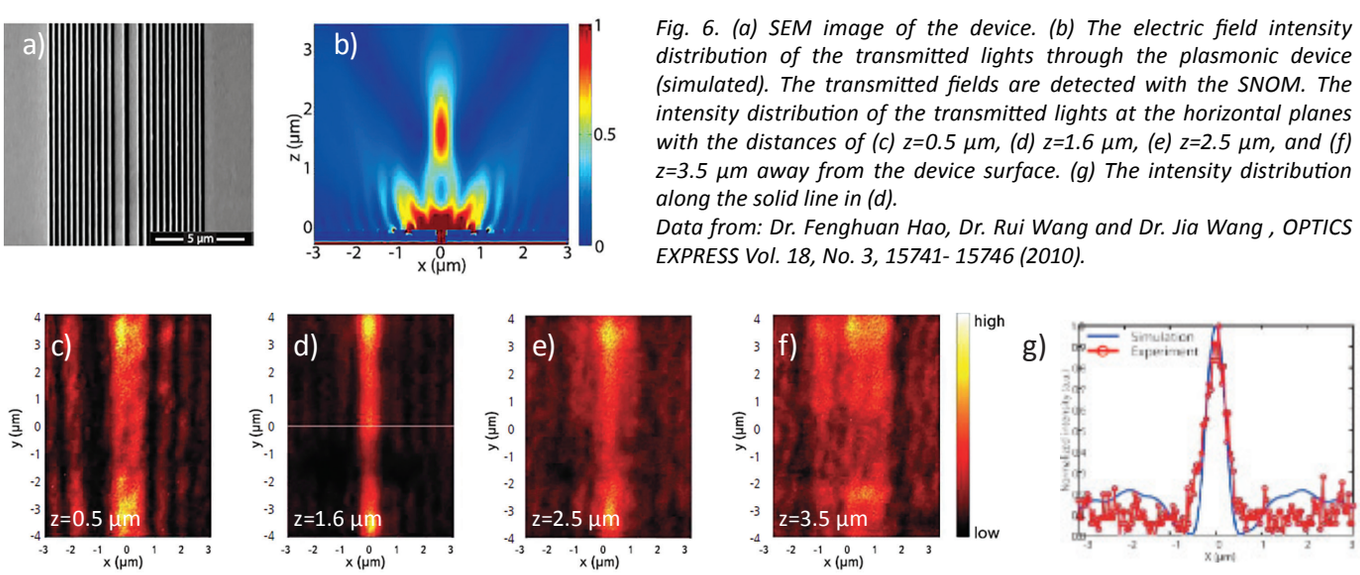

Fig. 6. (a) SEM image of the device. (b) The electric field intensity distribution of the transmitted lights through the plasmonic device (simulated). The transmitted fields are detected with the SNOM. The intensity distribution of the transmitted lights at the horizontal planes with the distances of (c) z=0.5 μm, (d) z=1.6 μm, (e) z=2.5 μm, and (f) z=3.5 μm away from the device surface. (g) The intensity distribution along the solid line in (d).
Data from: Dr. Fenghuan Hao, Dr. Rui Wang and Dr. Jia Wang , OPTICS EXPRESS Vol. 18, No. 3, 15741- 15746 (2010).

Light Spot Narrowing by an Assymetric Axicon

Diffraction of a Gaussian beam by axicons is studied by SNOM. Binary diffraction axicons with the period close to the light wavelength are formed by electron beam lithography on a quartz substrate. Different axicon geometries are studied. It is shown experimentally that asymmetric microaxicon can reduce the spot size of central light beam along polarization direction in a near zone of diffraction – overcoming the diffraction limit.

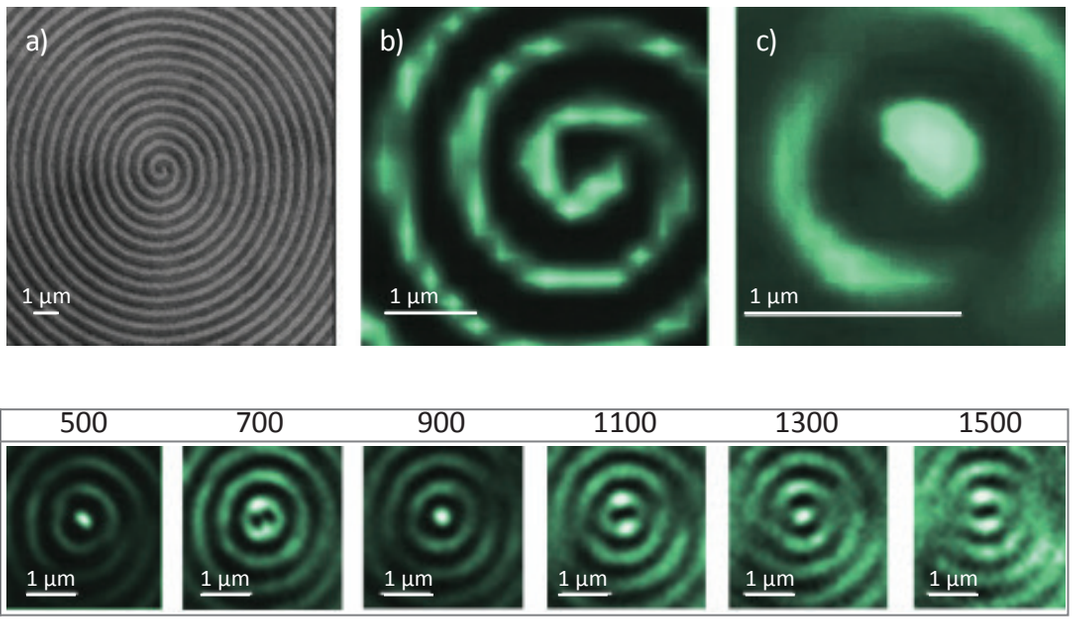

Fig. 7.(a) SEM image of the central part of a spiral axicon. (b) The diffracted light intensity distribution detected by SNOM in close proximity to the surface. (c) SNOM intensity distribution taken at ~500 nm from the surface. The central part of the beam at this plane is compressed in a light polarization direction (vertical) and has size less than optical limit. (d) Series of intensity distribution: the height of a scanning plane was varied from 500 nm to 1500 nm.
Data from: S. N. Khonina, D. V. Nesterenko, A. A. Morozov, R. V. Skidanov, and V. A. Soifer, OPTICAL MEMORY AND NEURAL NETWORKS, Vol. 21, No. 1, 17-26 (2012).

Focusing of a Radially Polarized Beam by a Solid Immersion Lens

Radially polarized beam focused by a solid immersion lens (SIL) is studied by SNOM. It delivers a laser spot beyond the diffraction limit demonstrating better focusing properties than a common linearly polarized beam.

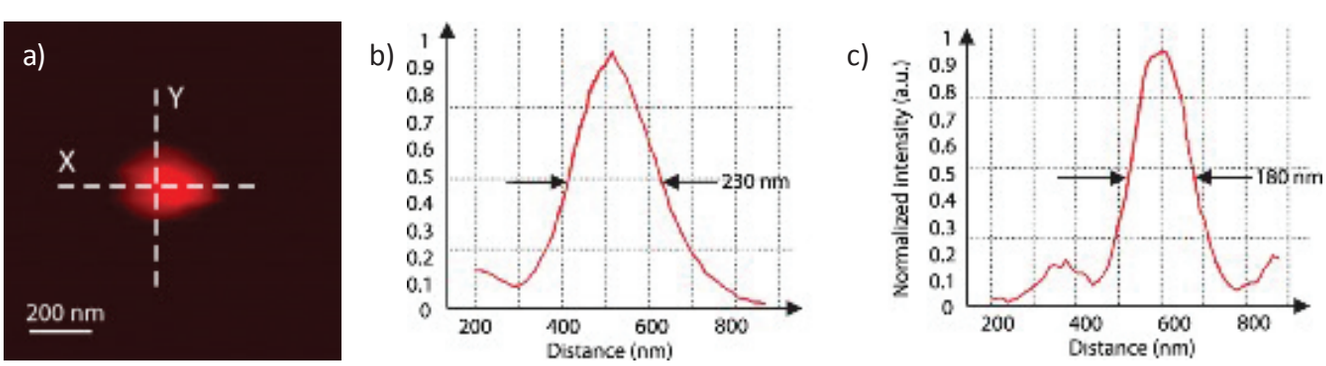

Fig. 8. Measured focus spot by a solid immersion lens with incident annular radially polarized beam, i.e., evanescent Bessel beam: (a) intensity distribution on the SIL bottom surface; (b) intensity along the X direction. The FWHM is 230 nm; (c) intensity along the Y direction. The FWHM is 180 nm. Size of the spot in both X and Y direction are considerably less than diffraction limit. Laser wavelength 633 nm.
Data from: Qing Li, Jia Wang, Jiying Xu, Jiefeng Xi and Guofan Jin, OPTICAL REVIEW Vol. 13, No. 4 283–287 (2006).

Color Separation in the Fresnel Diffraction Region of Rectangular Grating

Color separation of the incident light in the Fresnel diffraction region is a novel function of high-density dielectric rectangular gratings. Light of different wavelengths has different diffraction periods in the Z direction. For example, at 4.2 µm distance from the surface, position of intensity maximum for red excitation laser corresponds to position of intensity minimum for blue excitation laser - a spatial light separation occurs.

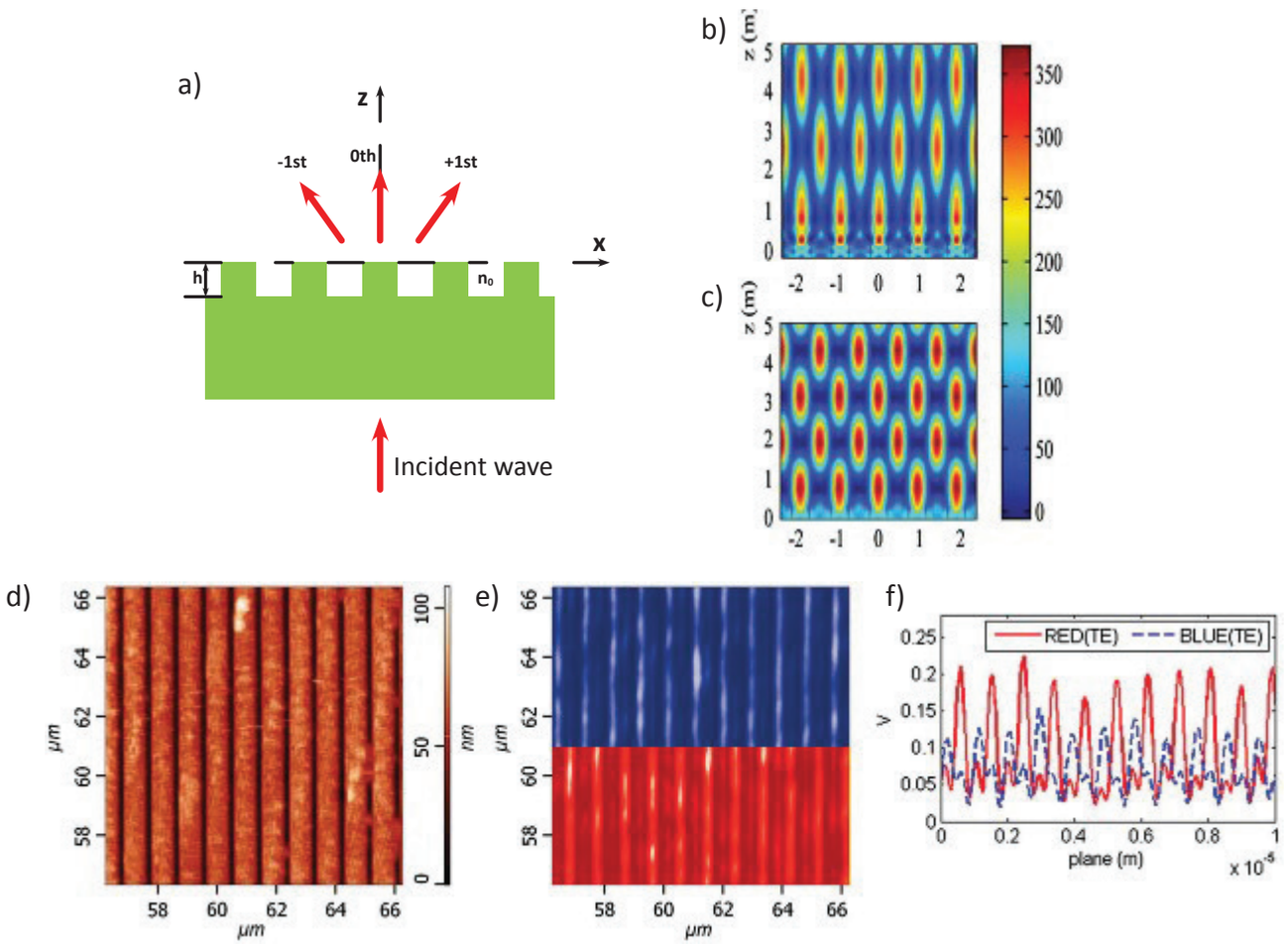

Fig. 9. (a) Schematics of the fabricated grating. The period of the grating is 1.5 λ (λ = 633 nm), and the duty cycle is 0.5. (b), (c) Calculated diffraction distributions for different incident wavelengths: 488 nm and 633 nm correspondingly. (d) The shearforce topography of the grating. Experimental results scanned by SNOM at z = 4.2 µm: (e) the field distribution with the incident laser wavelength 633 nm (bottom half) and 488 nm (top half), and (f) the intensity distribution at the same cross section for different wavelength of the incident laser.
Data from: Yue Fang, Qiaofeng Tan, Mingqian Zhang and Guofan Jin, APPLIED OPTICS, Vol. 51, No. 12, 2172-2177 (2012).

SNOM FOR PLASMONICS

SNOM is traditionally used to examine the Surface Plasmon Polaritons (SPP) behavior with high spatial resolution in all three dimensions (XYZ).

Plasmonic Fan-Out

SPP behavior is often studied in relation to conventional optical devices such as beam splitters and waveguides. The work conducted by Wang et al. (Fig. 10) realizes traditional fan-out optical arrangement in a plasmonic device. An optical fan-out element typically splits a single wave into plane waves by using gratings and lenses to generate an array of light spots.

A plasmonic fan-out array is generated by the structure shown in Fig. 10 (a, b). The device is produced using arrays of slits on a metal film, the slits being of less than the wavelength dimensions of the initial light. The structure consists of a 100 nm silver film deposited on a quartz substrate. The slit arrays are cut into the silver film by electron beam lithography (EBL) at a width of 265 nm to generate the highest surface plasmon response. The near field characteristics of the SPP pattern are investigated by SNOM with an aluminium coated fiber tip. The results of the imaging analysis are shown in Fig. 10 (c).

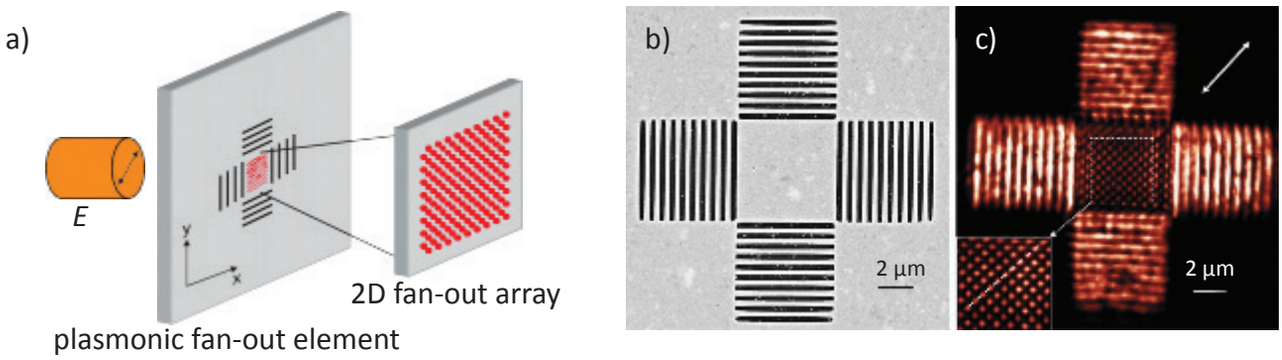

Fig. 10. (a) Subwavelength slit arrays are used to generate SPP waves propagating along the metal surface and four perpendicular counter-propagating SPP waves interfered each other to form the localized plasmonic dots array. (b) SEM image of subwavelength slit arrays structure. (c) 2D Near field image of electrical field distribution for diagonal polarization direction. Inset is the SPP field intensity distribution of the structure's centre area. The white arrow indicates the incident polarization direction. Excitation laser wavelengthis 633 nm.
Data from: Wang Qian, Jing Bu, X.-C. Yuan, OPTICS EXPRESS, Vol. 18, No. 3, 2662-2667 (2010).

Generation of Plasmonic Moiré Fringes Using Phase-engineered Optical Vortex Beam

The work demonstrates the dynamic generation of two dimensional (2D) plasmonic Moiré fringes resulting from the overlapping of two Surface Plasmon Polaritons (SPP) standing waves with an angular misalignment. The SPP waves are excited by an optical vortex (OV) beam with different topological charges (l= ±6). The sign of l determines handedness of the helical wave front. Due to their unique phase properties, OV beams provide a natural and simple phase modulation method to effectively and dynamically manipulate SPPs.

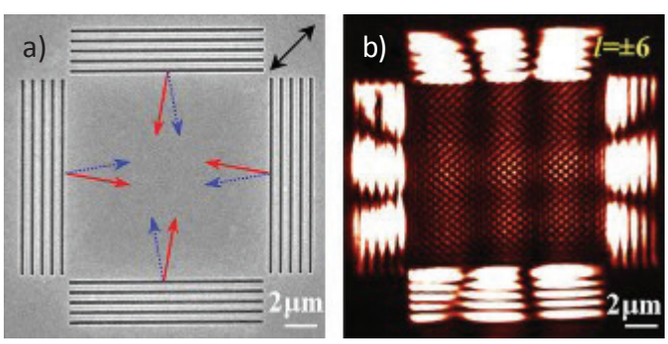

Fig. 11. (a) SEM image of four metallic gratings to generate plasmonic Moiré fringes. Black arrow shows the polarization direction of incident optical vortex beam. Red and blue arrows show the propagation direction of SPP excited by positive and negative topological charge optical vortex beams, respectively. (b) SNOM measured Moiré fringes resulting from overlapping of the two SPP standing waves.
Data from: Guanghui Yuan, Qian Wang, and Xiaocong Yuan, OPTICS LETTERS, Vol. 37, No. 13, 2715-2717 (2012).

Guided Plasmons on a Gold Waveguide

Surface plasmon polariton (SPP) propagation in an SPP waveguide is studied using SNOM equipped with a heterodyne interferometer. Both intensity and phase distribution of SPP electromagnetic field are measured.

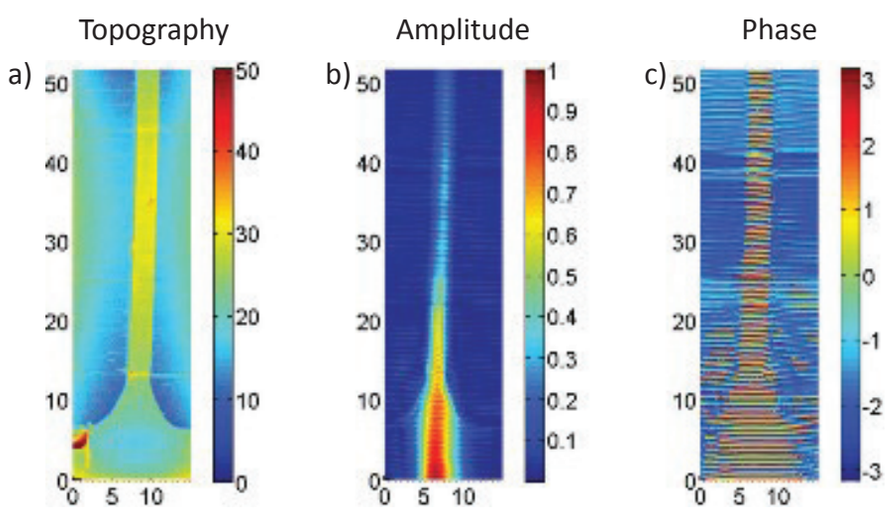

Fig. 12. (a) Topography of the waveguide. (b) Amplitude of the electromagnetic field coupled by SNOM probe. (c) Phase of the electromagnetic field. 785 nm excitation laser is used.
Data from: Antonello Nesci and Olivier J.F. Martin.

SERS Substrate

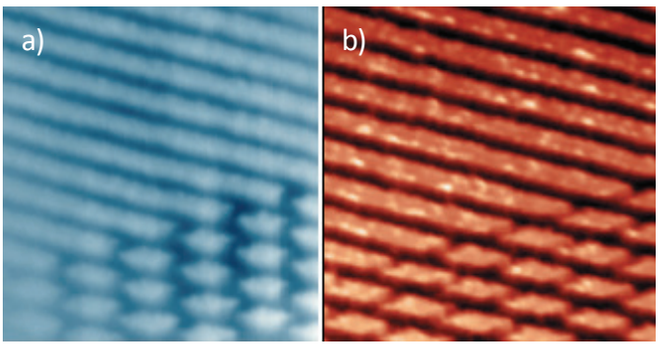

Fig. 13. SERS substrate – Au nanodiamond array on quartz. (a) AFM topography and (b) SNOM image, transmission mode. Period of the structure: 200 nm. Resolution of SNOM image: ~50 nm.
Data from: I. Arkov, E. Kuznetsov, NT-MDT SI.
Sample courtesy: Henrik Schneidewind, Institute of Photonic Technology (IPHT Jena), Germany.

Polarization-Controlled Tunable Directional Coupling of Surface Plasmon Polaritons

The polarization states of the optical signal that can be coupled to a plasmonic device are often limited by the selectivity of the coupling process. For directional SPP excitation, usually only the component of the incident light that is polarized perpendicularly to either groove- or ridge-like scattering elements (in the case of gratings) or to the metal surface itself (in the case of prism-based schemes) can be coupled into SPPs . Light in the orthogonal polarization does not couple to SPPs, leading to a decrease in the SPP signal and a loss of information about the incident polarization state.

Additional challenges arise in controlling the direction of propagation of the generated SPPs. Usually the direction of propagation of generated SPPs is difficult to control, that results in a substantial source of noise and reduces efficiency. This work presents a directional plasmonic coupler that addresses these challenges by offering polarization-invariant coupling efficiency to SPPs while allowing full control over the distribution of power between two counter-propagating SPP modes. This includes unidirectional coupling and preserves polarization information. A special structure was fabricated in a 150-nm-thick gold film using focused ion beam milling (FIB). The structure was backilluminated with polarized 633-nm laser light, and the SPPs were measured using scanning near-field optical microscopy.

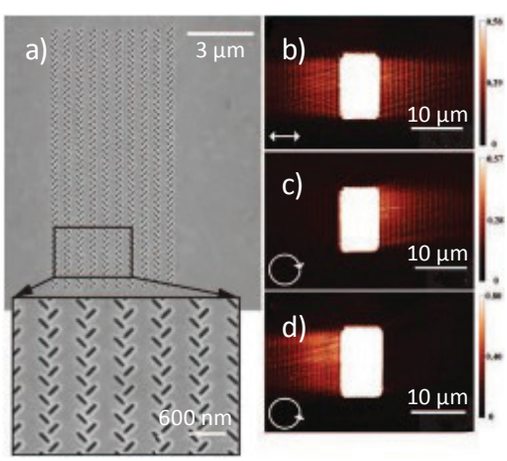

Fig. 14. Surface plasmon polaritons (SPP) formed by coupler structure: (a) SEM image of a structure fabricated in a gold film for operation at λ=633 nm. SNOM images of the structure backilluminated by light with different polarizations (b) linear, (c) right circular, (d) left circular.
Data from: Jiao Lin, J. P. Balthasar Mueller, Qian Wang, Guanghui Yuan, Nicholas Antoniou, Xiao-Cong Yuan, Federico Capasso, SCIENCE, Vol. 340 , 331-334 (2013).

SNOM FOR PHOTONIC CRYSTALS

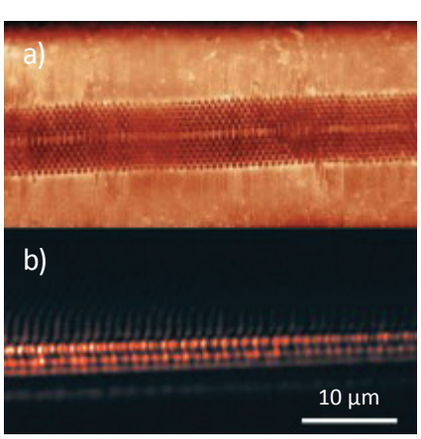

Light Propagation in a Photonic Crystal Waveguide

Aperture-SNOM in collection mode is used to correlate the electromagnetic field distribution with the surface topography of the photonic crystal. The optical near-field confined above the sample surface is collected by a SNOM tip, placed several nanometers above the sample surface.

Fig. 15. Light propagation in a one-line-defect photonic crystal (PhC) waveguide patterned into a 450 nm thick free-standing lithium niobate membrane. SNOM topography (a) and optical near-field (b) images recorded above the surface of the PhC waveguide. The Bloch wave vectors of the PhC waveguide can be retrieved from optical near-field images.
Data from: R. Geiss, S. Diziain, N. Janunts, APPLIED PHYSICS LETTERS 97, 131109 (2010).

Analysis of Slow Bloch Modes in a Photonic Crystal

The photonic crystal is prepared by drilling a honeycomb lattice of air holes in the InP slab using e-beam lithography followed by reactive ion etching. Near-field optical microscopy is used to visualize the evanescent component of the mode with a spatial resolution below the diffraction limit.

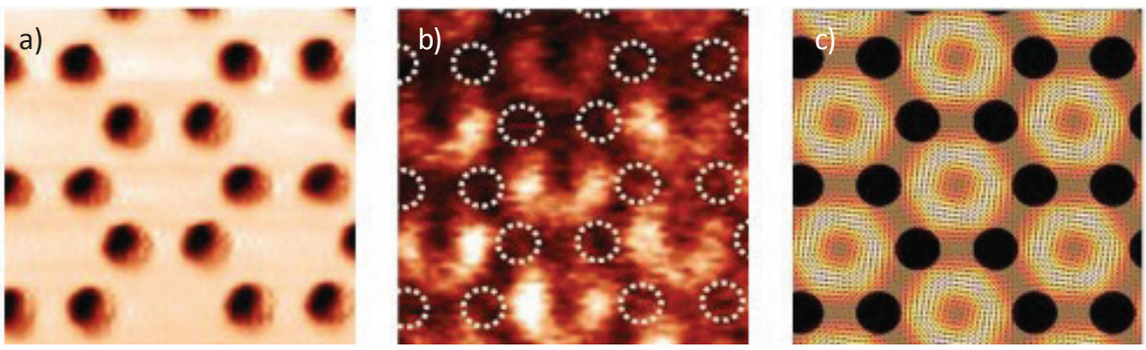

Fig. 16. (a) Shear-force topographic image (2×2 µm). (b) Optical near-field image at 1611 nm (2×2 µm), circles indicate holes positions of the 2D-Photonic crystal. Doughnut-shaped monopolar modes in each unit cell are observed, having the inner and outer radiuses 70 nm and 310 nm correspondingly. (c) Simulated electrical field intensity at the surface of the photonic crystal (2×2µm).
Data from: Thanh-Phong Vo, Adel Rahmani, Ali Belarouci, Christian Seassal, Dusan Nedeljkovic and Ségolène Callard, OPTICS EXPRESS, Vol. 18, No. 26, 26879-26886 (2010).

SNOM FOR PHOTOVOLTAICS

Localized SNOM Excitation for Solar Cell Studies

SNOM is used for localized optical excitation of a monocrystalline silicon solar cell. Topography, local surface reflection and localized photoresponse of the cell are simultaneously mapped while scanning with the SNOM probe. This allows characterizing near-surface defects and other optoelectrical properties of the cell with high spatial resolution and correlating them with the surface topography.

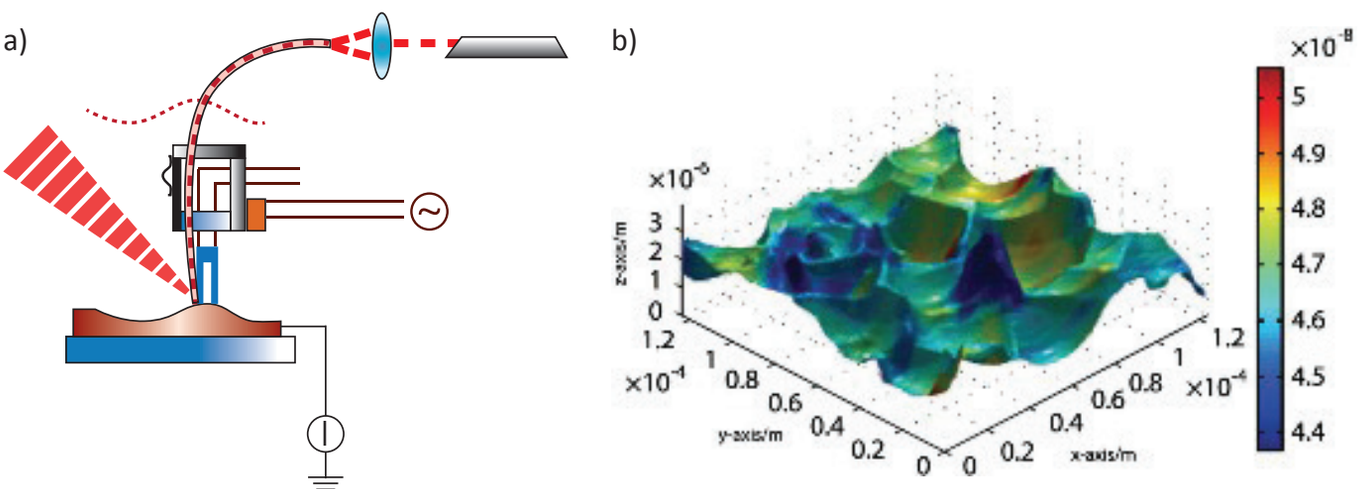

Fig. 17. (a) Scheme of setup. (b) Overlay of sample topography (3D surface profile) and localized photo-induced current (color scale).
Data from: P. Tománek, P. Škarvada, R. Macků, and L. Grmela, Advances in Optical Technologies, Volume 2010, Article ID 805325 (2010).

SNOM FOR POLYMERS

Perylene Embedded in Polyfluorene

Perylene (a small-molecular organic semiconductor) was embedded in Polyfluorene (PFO) polymer organic semiconductor thin film forming a rhombus structure. SNOM transmission spectroscopy scheme was used to study the optical proprieties of the structure. It is known that fluorescence properties of perylene nanosheets directly relate to their crystal structures. For β-phase rhombus perylene, the fluorescence peak is around 620 nm, which can be clearly observed from fluorescent spectra along the section on the SNOM image. Excitation laser wavelength was 473 nm.

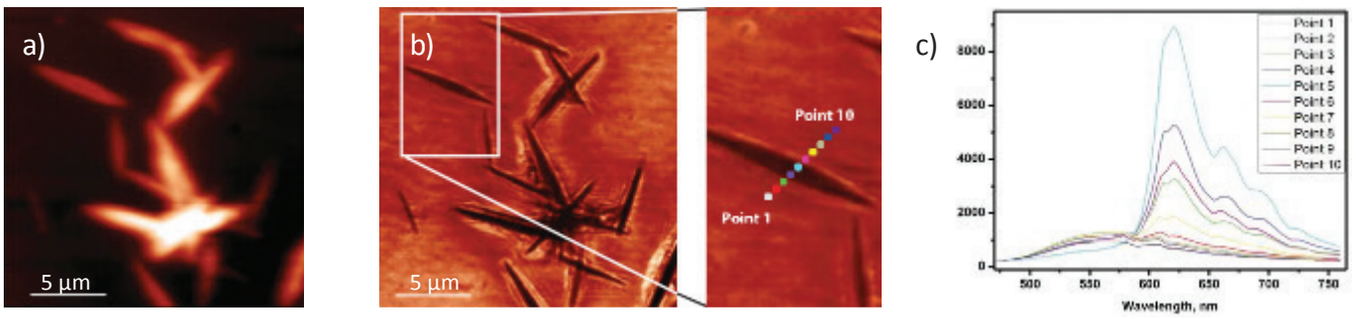

Fig. 18. (a) AFM image of Perylene embedded in PFO. (b) SNOM transmission image. (c) Fluorescent spectra for 10 points of section from the SNOM image. Data from: E. Kuznetsov, S. Timofeev, NT-MDT SI.Sample courtesy: Xinping Zhang, Beijing University of Technology, College of Applied Sciences.

SNOM FOR QUANTUM DOTS

For high resolution photoluminescence (PL) studies of quantum dots (QDs) grown on non-transparent substrate the so-called illumination-collection SNOM regime is most efficient. In this regime, both laser illumination and PL signal collection are performed through the same SNOM probe nano-aperture. Proper design of the probes (high transmission), optimized experimental setup (good collection optics) as well as right measuring procedure (ensuring that probe is in near-field optical regime with the sample) allow efficient optical excitation and detection of individual QD PL.

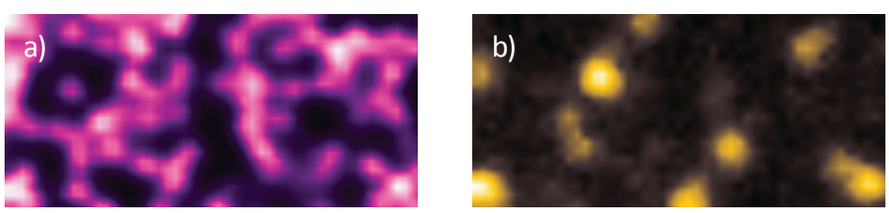

Fig. 19. SNOM photoluminescence images of self-assembled InP/GaInP quantum dots on GaAs substrate at two different PL wavelength bands: (a) λ ≈ 740 nm, (b) λ ≈ 800 nm. The first PL band (a) correspond to "small" QDs, ~20-50 nm diameter. The second PL band (b) corresponds to "large" QDs, ~100-200 nm diameter. Individual QDs of different sizes are clearly detected on SNOM images. Their PL spectra were also measured. Size of scans: 1x2 µm. Data from: A. Ankoudinov, A. Mintairov, A. Shelaev, Ioffe Institute & NT-MDT SI.

SCATTERING (APERTURELESS-) SNOM

Scattering (apertureless) SNOM technique is usually used to visualize localized electromagnetic field in plasmonic structures. In this technique, a sharp probe is used to scatter localized near-field light into the far field. The scattered radiation intensity is measured in far field while tip scans over the sample surface, thus visualizing distribution of light localized in the structure with spatial resolution ~10 nm.

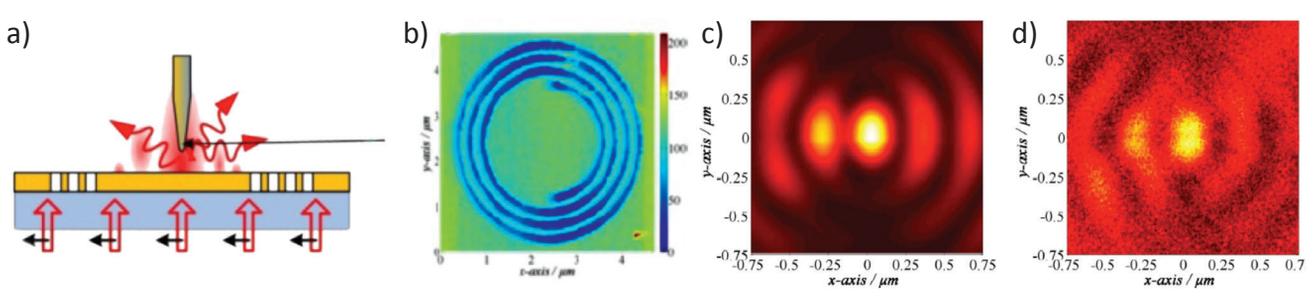

Fig. 20. (a) Scattering SNOM is used to visualize longitudinal field distribution (|Ez|2) in a plasmonic lense (PL). (b) AFM image of the PL structure – circle slits in a thin Au film on a glass substrate. (c) Calculated and (d) measured longitudinal field intensity in the center of the PL.

NT-MDT SI SNOM SPECIFICATION

SNOM & other probes
SNOM optical fibers; SNOM apertured cantilevers; All types of AFM cantilevers; Sharp metal wires

Supported standard modes
SNOM modes: Transmission; Collection; Reflection; HybriD mode (optical signal vs. tip-sample distance recording) for multi-dimentional optical imaging

AFM modes*: >30 modes (MFM, SKM, SCM, SRI, LFM, EFM, SThM, UFM, PFM, AFAM and others)

Detected optical signals
Laser intensity; Fluorescence intensity; Spectroscopy (full spectrum at each point)

Excitation/detection wavelength range
400 – 1700 nm; Customized solutions for wider ranges are possible

Advanced near-field modes and techniques
Scattering SNOM (s-SNOM); Apertureless SNOM (a-SNOM); Tip Enhanced Raman Scattering (TERS); Tip Enhanced Fluorescence Spectroscopy (TEFS); SNOM lithography (vector, raster); Light emission/ absorption at AFM/STM gap; Polarization microscopy

Optical detectors
Photon multipliers (VIS, IR); Spectrometer with TE cooled CCD camera; Avalanche photodiodes (photon counting regime)

Scanning and feedback mechanisms
Scan by tip & scan by sample regime (100 x 100 µm) High resonance XYZ piezotube for fast scanning (closed-loop feedback); Flat piezo-driven scanning stage (closed-loop feedback)

Laser based cantilever deflection detection (VIS or IR laser); Quartz tuning fork resonator force detection system (shear force & normal force regimes)

Other features
Easy upgrade/integration with confocal Raman/Fluorescence microscopy

Automated alignment of laser spot to aperture of SNOM cantilever

Very high efficiency (numerical aperture) excitation/collection optics

Environmental control: temperature, humidity, gases, liquid, magnetic field

Compatible with commercially available inverted optical microscopes

**May require different types of probes. When probes are exchanged, exact area of the sample is kept within µm precision*

NT-MDT Spectrum Instruments
www.ntmdt-si.com